LA-UR-83-1197

Conf-830538--4

Los Alamos National Laboratory is operated by the University of California for the United States Department of Energy under contract W-7405-ENG-36.

LA-UR--83-1197

DE83 011148

TITLE: EVALUATION OF THE STREAMING-MATRIX METHOD FOR DISCRETE-ORDINATES DUCT-STREAMING CALCULATIONS

AUTHOR(S): Bradley A. Clark, W. T. Urban, and Donald J. Dudziak

SUBMITTED TO: Sixth International Conference on
Radiation Shielding
Tokyo, JAPAN
May 16-20, 1983

Los Alamos National Laboratory
Los Alamos, New Mexico 87545

EVALUATION OF THE STREAMING-MATRIX METHOD FOR DISCRETE-ORDINATES DUCT-STREAMING CALCULATIONS

Bradley A. Clark, W. T. Urban, and Donald J. Dudziak
Los Alamos National Laboratory
University of California
Los Alamos, New Mexico, USA

ABSTRACT

A new deterministic streaming technique called the Streaming Matrix Hybrid Method (SMHM) is applied to two realistic duct-shielding problems. The results are compared to standard discrete-ordinates and Monte Carlo calculations. The SMHM shows promise as an alternative deterministic streaming method to standard discrete-ordinates.

INTRODUCTION

Neutron shielding problems are usually analyzed with computers using either the discrete-ordinates or Monte Carlo technique; often both are required. Since many of these problems include voids, ray effects limit the accuracy of discrete-ordinates calculations. However, when detailed flux or reaction-rate distributions are required, discrete-ordinates is the only method that provides those results with reasonable computing times.

In this paper, a new deterministic streaming technique, called the Streaming Matrix Hybrid Method (SMHM), is applied to two multigroup shielding problems. Results for the SMHM are compared with standard discrete-ordinates and Monte Carlo solutions.

The remainder of the paper is organized in four parts. First, we give a brief description of the theory behind the SMHM and its implementation in the discrete-ordinates code TRIDENT-CTR. The second section describes the two problems that are analyzed. Also, the solution techniques used for the SMHM, standard discrete-ordinates, and Monte Carlo calculations are described. The third section contains a description of the results of the analyses. Finally, we give our conclusions concerning the potential of the SMHM.

THEORY

The SMHM is a hybrid method in the sense that two transport methods are used in the same calculation. The streaming matrix calculates particle streaming through selected voids; standard discrete-ordinates methods are used in the remainder of the problem. A detailed description of the theory behind the SMHM is available elsewhere;[1,2] a brief summary is presented here.

The streaming matrix calculates transport through a void that may contain an inhomogeneous source. Streaming is calculated by solving the integral transport equation to compute "view factors" in the phase space that includes the discrete-ordinates angular variables. The calculation is not restricted to the discrete-ordinates quadrature points. Discrete-ordinates angular fluxes are used to define the flux on the void surface throughout the entire angular range. Continuous treatment of the azimuthal angle ensures that angular redistribution during streaming is calculated analytically. Many η ($\eta=\Omega_z$) values are used to reduce the z component of the ray effect. Each of these η values is called a sublevel, motivated by the usual arrangement of discrete-ordinates quadrature sets on η levels in curvilinear geometries. The accuracy of streaming matrix calculations depends on the number of η sublevels. Exiting angular fluxes are normalized to preserve particle balance. The normalized phase space "view factors" are arranged into a matrix that couples entering angular fluxes to exiting angular fluxes.

The SMHM is implemented in the triangular mesh discrete-ordinates code TRIDENT-CTR.[3] Additional input describes regions that are to be treated using the SMHM. The Streaming Matrix (SM) is calculated before the inner/outer iteration procedure begins. The SM is saved on disk and may be reused for problem restarts and other problems containing the same void shape.

Previous results on simple one-group streaming problems indicate that when an adequate number of η sublevels and sufficient discrete-ordinates quadrature order are used, scalar fluxes within 5% of Monte Carlo values are obtained. Application of the SMHM to more difficult multigroup problems is the subject of the remainder of this paper.

TEST PROBLEMS

Past testing of the SMHM was limited to simple one-group void problems; those results indicated the need for further testing of the method on more complex multigroup duct problems. Two such problems have been selected for analysis. They are modeled such that differences between the discrete-ordinates multigroup data and the continuous formulation in the Monte Carlo code MCNP[4] are minimized. The two problems are the Cylindrical Duct Problem (CDP) and the Annular Duct Problem (ADP). These problems are analyzed using the standard discrete-ordinates method, the Monte Carlo method, and various SMHM calculations.

Cylindrical Duct Problem

The geometry of the CDP is described in Figure 1. The problem is symmetric in r-z geometry. A central duct ($0 \leq r \leq 5$ cm, $0 \leq z \leq 100$ cm) is treated using the SMHM; its L/D ratio is 10. The duct is lined with 2 cm of 316 stainless steel (SS-316); the composition by weight is: 63% Fe, 18% Cr, 14% Ni, 3% Mo, and 2% Mn. The major portion of the shield (7 cm $\leq r \leq$ 27 cm, $0 \leq z \leq$ 100 cm) is a mixture of 20% (by volume) water and 80% SS-316. On top of this is a void ($0 \leq r \leq$ 27 cm, 100 cm $\leq z \leq$ 102 cm) that is not treated with the SMHM. ENDF/B-V cross sections are used throughout.

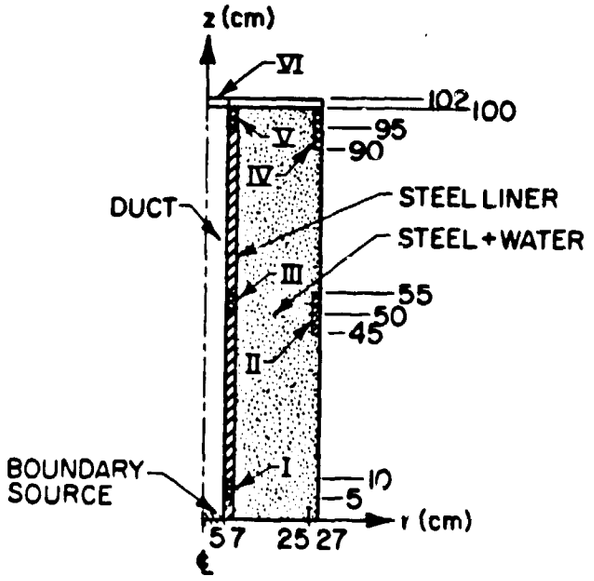

Fig. 1. Cylindrical Duct Problem. Roman numerals indicate edit zones used for average flux comparisons.

An isotropic (for $\Omega_z > 0$) angular flux boundary source distributed uniformly at $z = 0$ and $0 \leq r \leq 5$ cm drives the problem; it emits neutrons in the energy range of the second discrete-ordinates energy group (13.5-15.0 MeV). Edit zones labeled I through VI are shown in Fig. 1. The average scalar flux is calculated in each of these zones for the source-energy group; an energy-integrated value is also computed.

Details of the models used for each of the transport methods are contained in the following sections.

Discrete-Ordinates Model

The geometric model of the cylindrical shield penetrated by a simple cylindrical duct, shown in Fig. 1, is represented exactly in TRIDENT-CTR. The spatial mesh consists of 20 equally spaced bands in $0 \leq z \leq 100$ cm, and one band in the top 2-cm void region. For edit purposes, the outermost zone is subdivided at $r = 25$ cm into two zones. The resulting four zones are assigned 9, 2, 8, and 2 triangles per band, respectively. Neutron cross sections for the two material compositions are premixed from ENDF/B-V data in the Los Alamos standard 30-group structure.[5]

All discrete-ordinates calculations, with the exception of two S_{16} cases discussed below, use S_8 quadrature (EQ_8)[6] and transport-corrected[7] P_3 scattering cross sections. Pointwise convergence is, in all cases, within 4×10^{-4}. Results presented below are computed using various numbers of n sublevels. In all cases, the minimum and maximum values of n are 10^{-5} and 0.99999, respectively. A spatially uniform surface source is specified for the bottom surface of the duct, with a cosine angular source distribution relative to the duct axial direction (isotropic angular flux distribution) on each surface segment.

Edit regions are defined as shown by Roman numerals in Fig. 1. In addition to I and V in Fig. 1, edit regions are defined every 5 cm along the steel liner in order to obtain a detailed spatial flux distribution for comparison with Monte Carlo calculations.

Monte Carlo Model

Calculations are made using MCNP,[4] for the configuration shown in Fig. 1. These results are the reference values used for comparison with standard TRIDENT-CTR and SMHM calculations.

The MCNP model s identical to the configuration illustrated in Fig. 1. MCNP is modified to sample the boundary source, i.e., a spatially uniform circular plane source from which the neutrons are emitted with a cosine angular distribution and a uniform energy distribution between 13.5 and 15.0 MeV. No spatial, energy, or angular biasing is incorporated into the source sampling. Propagation of the neutrons from the source to the regions of interest is enhanced through the use of geometry splitting and Russian roulette. Neutron fluxes are obtained with volumetric track length estimators and point detectors. A sufficient number of neutron histories are followed to calculate neutron fluxes at the exit of the duct with fractional errors less than 0.01 and 0.10 as determined by the point detector and volumetric track length estimators, respectively. Fractional errors presented in this report are at the 68% confidence level.

Annular Duct Problem

The ADP is similar to the CDP except that the major duct is annular (22 cm $\leq$ r $\leq$ 27 cm and 0 $\leq$ z $\leq$ 100 cm); the duct is lined with 2 cm of SS-316. Again, the bulk of the shielding is a 20% (by volume) water and 80% SS-316 mixture. The compositions are the same as in the CDP.

An isotropic angular flux boundary source ($\Omega_z > 0$) at z = 0 and 22 cm $\leq$ r $\leq$ 27 cm drives the problem; it is nonzero only in the second discrete-ordinates energy group. Edit zones labeled I-XI are shown in Fig. 2. Average scalar fluxes are computed in these zones for the source group as well as the energy-integrated average.

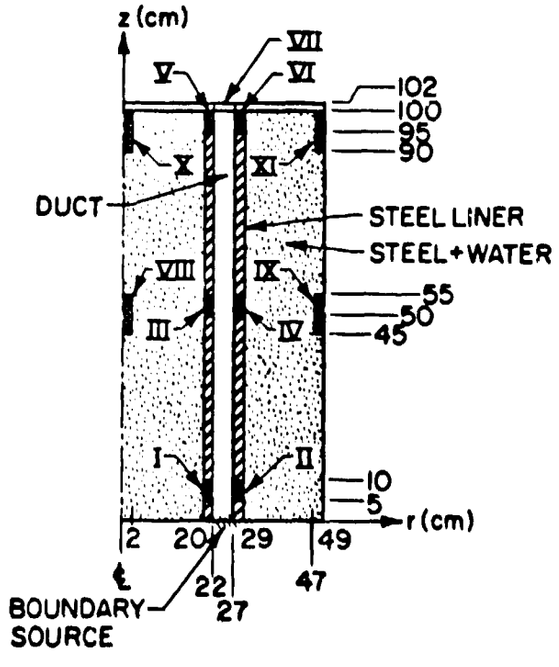

Fig. 2. Annular Duct Problem. Roman numerals indicate edit zones used for average flux comparisons.

Details of the models used for each of the transport methods are contained in the following sections.

Discrete-Ordinates Model

The geometric model of the cylindrical annulus penetrating a cylindrical shield, as shown in Fig. 2, is represented exactly in TRIDENT-CTR. Seven zones are specified, with the radii shown along the r-axis in Fig. 2. The innermost and outermost zones are added strictly for editing purposes in the regions designated by Roman numerals. The seven zones contain 2, 9, 2, 5, 2, 9, and 2 triangles per zone, respectively. All other specifications such as order of quadrature, convergence, number of n sublevels, cross sections, etc., are as given above for the simple cylindrical duct.

Monte Carlo Model

The MCNP calculation for the annular duct problem is based on the geometric model shown in Fig. 2. Compositions used are those described earlier. MCNP is modified to sample the annular disk boundary source, i.e., spatially uniform annular plane source from which neutrons are emitted with a cosine angular distribution and a uniform distribution of energies between 13.5 and 15.0 MeV. No spatial, energy, or angular biasing is used in the source sampling. The variance reduction technique employed in the transport process and the fractional error goals in this calculation are the same as described for the cylindrical duct MCNP calculation.

RESULTS

The results for each configuration and method take the form of neutron fluxes averaged over volumetric regions plus a single pointwise value at the duct exit. Fluxes reported are the source-group and total neutron fluxes.

The MCNP results are the reference values against which the deterministic results are evaluated. When the uncollided MCNP flux at the point detector at the cylindrical duct exit is compared with previous calculations and the analytic solution, the agreement is within 2%, thereby providing confidence in the MCNP results.

Cylindrical Duct Problem

The results for the cylindrical duct problem are presented in Table 1. This table contains the MCNP results and the results of three TRIDENT-CTR calculations; one with the SMHM, and one each using standard discrete-ordinates with S_8 and S_{16} quadrature sets. Ratios of each of the deterministic results to the MCNP results are also presented. Examination of these data yields the following observations: (a) in region I, all of the TRIDENT-CTR results are in good agreement with MCNP, particularly for the source-group flux; (b) proceeding up the inner steel liner, regions III and V, the SMHM results get progressively larger than the MCNP results, and the standard TRIDENT-CTR results exhibit the ray effect and are smaller than the corresponding MCNP results near the duct exit; and (c) at the end of the duct the SMHM results slightly underpredict the MCNP results and the standard TRIDENT-CTR results severely underpredict the MCNP flux. Along the steel liner, these calculations indicate that the standard TRIDENT-CTR results with S_{16} have errors no greater than the SMHM results. However, at the duct exit, region VI and the point within this region, the standard S_{16} results underpredict the source-group fluxes by a factor of 60, while the total flux is underpredicted by a factor of 4. Thus, ray effects are clearly evident at the duct exit for the S_{16} and S_8 results. Fig. 3 shows the fall-off of the S_{16} and SMHM results along the duct wall, with the strong divergence beginning at ≈ 80 cm. At the point above the duct exit, the ratio of the source-group flux to the total flux is 0.78 for MCNP, 0.68 for SMHM, but only 0.052 for the standard S_{16} calculation.

Figure 4 presents a comparison of the MCNP and SMHM source-group and total fluxes in the steel liner adjacent to the duct. These data clearly show the progressive overestimation of the liner fluxes by the SMHM as one moves farther from the source.

Table 1. Cylindrical Duct Problem Neutron Fluxes

Region	Source Group Neutron Fluxes				Flux Ratios		
	MCNP	TRIDENT-CTR			SMHM / MCNP	S_8 / MCNP	S_{16} / MCNP
		SMHM[d]	S_8	S_{16}			
I	2.07-3[a](0.0056)[b]	2.18-3	2.13-3	2.14-3	1.05	1.03	1.03
II	c	1.38-7	1.05-7	1.56-7	—	—	—
III	3.63-5(0.0402)	6.18-5	2.12-5	5.25-5	1.70	0.58	1.45
IV	c	9.05-9	3.21-10	5.19-9	—	—	—
V	7.55-6(0.0815)	1.65-5	5.84-8	3.43-6	2.19	$<10^{-2}$	0.45
VI	3.97-5(0.0571)	3.24-5	2.29-8	5.57-7	0.82	$<10^{-3}$	0.01
Pt.[e]	3.89-5(0.0046)	3.31-5	1.88-8	6.55-7	0.85	$<10^{-3}$	0.02

Region	Total Neutron Fluxes				Flux Ratios		
	MCNP	TRIDENT-CTR			SMHM / MCNP	S_8 / MCNP	S_{16} / MCNP
		SMHM[d]	S_8	S_{16}			
I	5.14-3(0.0071)	4.90-3	5.84-3	5.87-3	0.95	1.14	1.14
II	c	5.50-6	5.67-6	5.31-6	—	—	—
III	1.95-4(0.0175)	2.27-4	2.32-4	2.48-4	1.16	1.19	1.27
IV	c	4.29-7	5.77-8	2.87-7	—	—	—
V	1.96-5(0.0534)	3.74-5	4.27-6	1.79-5	1.91	0.22	0.91
VI	4.98-5(0.0466)	4.67-5	3.31-6	1.25-5	0.94	0.07	0.25
Pt.[e]	4.97-5(0.0082)	4.89-5	c	1.25-5	0.98	—	0.25

[a] 2.07-3 = 2.07×10^{-3}

[b] (0.0056) is the 1σ fractional error estimate.

[c] Value not calculated.

[d] SMHM values are for S_8 and 800 n sub-levels.

[e] Located at the duct exit, (r,z) = (0.4167 cm, 100.667 cm).

No single effect has been identified as the source of the differences between the two sets of calculations. However, some approximations in the SMHM calculations can be eliminated as significant sources of error based upon experience with similar systems. For example, the convergence is adequate, as is the S_8 quadrature for the non-streaming portion of the calculation. Similarly, the cross-section data base and group structure have been well tested,[8] and resonance self-shielding effects are minor. However, the SMHM approximation of a constant angular flux exiting the liner in each angular bin could introduce a significant error for fluxes entering the duct after scattering in the shield.

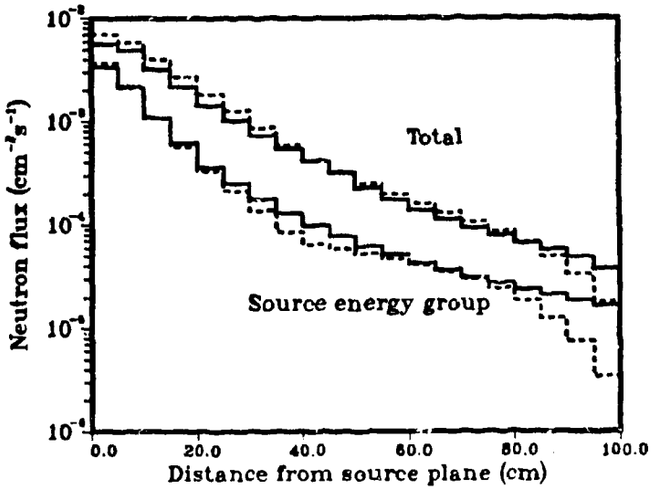

Fig. 3. Flux comparisons in the cylindrical duct steel liner as a function of distance from the source plane. (Solid line = SMHM, Dash line = S_{16}.)

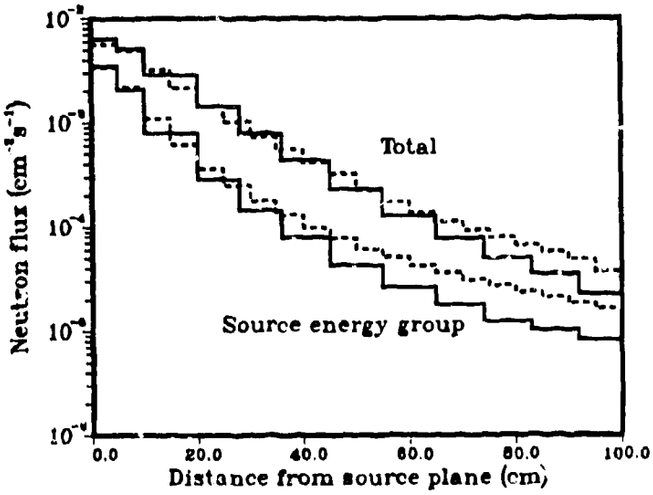

Fig. 4. Flux comparisons in the cylindrical duct steel liner as a function of distance from the source plane. (Solid line = MCNP, Dash line = SMHM.)

For regions II and IV in Fig. 1, at the outer edge of the cylindrical shield, the three deterministic calculations show variations attributable to the differing surface sources along the duct walls. Region II has a relatively small variation (≈24% in the source group and ≈3% in total flux) relative to the SMHM results, as would be expected from the relatively good agreement among SMHM, S_8, and S_{16} fluxes in the lower portion of the duct wall. Conversely, region IV shows large flux variations, an order of magnitude in both the source-group and total fluxes for S_8, due to the large errors in flux on the upper duct wall liner.

Annular Duct Problem

Results for the annular duct calculation are presented in Table 2. Analysis of these data yields observations similar to those obtained from the cylindrical duct data, except that the S_{16} results deteriorate more at the upper end of the annulus liner (regions V and VI). Although the SMHM to MCNP source-group flux ratios along the inner steel liner (regions I, III, and V) are of the same magnitude as observed for the cylindrical duct liner, the ratios for the outer liner are much better.

In both the inner and outer liners, the total fluxes show much better agreement than source-group fluxes. At the end of the annular duct, the SMHM underestimates the fluxes by a larger degree than in the CDP. These results are consistent with those observed in the CDP. In the ADP, the scattered component of the source-group flux is expected to be greater than in the CDP, lending support to the idea that cross-section differences may have a role in these errors. Although a direct comparison of the cross-section treatment in the two transport methods is complex, the reduction of the total and within-group scattering cross sections in the source-group by the Bell

Table 2. Annular Duct Problem Neutron Fluxes

Region	Source Group Neutron Fluxes				Flux Ratios		
	MCNP	TRIDENT-CTR			SMHM	S_8	S_{16}
		SMHM[e]	S_8	S_{16}	MCNP	MCNP	MCNP
I[a]	3.21-4[b](0.0121)[c]	2.92-4	2.93-4	2.92-4	0.91	0.91	0.91
II[a]	3.38-4(0.0095)	3.12-4	3.09-4	3.09-4	0.92	0.91	0.91
III	4.49-6(0.0560)	7.48-6	9.26-7	7.47-6	1.67	0.21	1.66
IV	1.53-5(0.0323)	1.63-5	2.41-6	1.45-5	1.07	0.16	0.95
V	8.70-7(0.0996)	1.99-6	3.03-9	7.08-8	2.29	$<10^{-2}$	0.09
VI	3.16-6(0.0653)	4.57-6	6.42-9	2.13-7	1.45	$<10^{-2}$	0.07
VII	1.06-5(0.0363)	6.09-6	2.80-9	1.14-7	0.57	$<10^{-3}$	0.01
Pt.[f]	1.08-3(0.0047)	6.67-6	2.47-9	9.91-9	0.62	$<10^{-3}$	$<10^{-2}$
VIII	d	1.34-7	7.49-8	1.87-7			
IX	d	5.26-8	4.84-8	6.29-8			
X	d	1.58-8	3.45-10	2.37-9			
XI	d	4.19-9	1.57-10	1.19-9			

Region	Total Neutron Fluxes				Flux Ratios		
	MCNP	TRIDENT-CTR			SMHM	S_8	S_{16}
		SMHM[e]	S_8	S_{16}	MCNP	MCNP	MCNP
I[a]	9.06-4(0.0120)	6.85-4	9.56-4	9.51-4	0.76	1.06	1.05
II[a]	9.05-4(0.0103)	7.04-4	9.50-4	9.46-4	0.78	1.05	1.05
III	6.90-5(0.0132)	4.73-5	5.71-5	8.08-5	0.69	0.83	1.17
IV	8.62-5(0.0134)	6.24-5	6.09-5	9.23-5	0.72	0.71	1.07
V	6.26-6(0.0271)	7.34-6	1.45-6	3.29-6	1.17	0.23	0.53
VI	1.01-5(0.0335)	1.12-5	1.60-6	4.26-6	1.11	0.16	0.42
VII	1.63-5(0.0248)	1.09-5	1.12-6	3.39-6	0.67	0.07	0.21
Pt.[f]	1.65-5(0.0068)	1.19-5	d	d	0.72	—	—
VIII	d	1.57-5	1.42-5	1.85-5			
IX	d	2.24-6	1.94-6	2.59-6			
X	d	1.30-6	1.83-7	5.55-7			
XI	d	1.96-7	2.33-8	8.03-8			

[a] MCNP region $5 < z < 8$ whereas TRIDENT-CTR region $5 < z < 10$ cm.

[b] $3.21\text{-}4 = 3.21 \times 10^{-4}$.

[c] 1σ fractional error estimate.

[d] Value not calculated.

[e] SMHM values are for S_8 and 800 n sub-levels.

[f] Located at the duct exit, (r,z) = (24.5 cm, 101.333 cm).

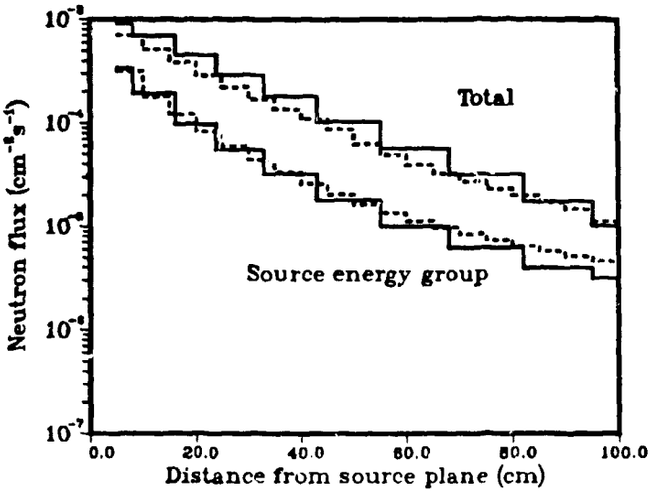

Fig. 5. Flux comparisons in the annular duct outer steel liner as a function of distance from the source plane. (Solid line = MCNP, Dash line = SMHM.)

et al. prescription[7] suggests this effect may be due, at least partly, to cross-section differences. A second source of these errors may be the constant-flux assumption for re-entering fluxes made by the SMHM. While this assumption is exact for the source-group boundary source, it is clearly inaccurate for scattered fluxes.

In regions VIII, IX, X, and XI, the results are analogous to those in the outer regions of the CDP. That is, in the lower regions, VIII and IX, the agreement of both source-group and total fluxes is reasonable in view of the accuracy of the respective fluxes in the lower portion of the annular duct liner. However, for regions X and XI the agreement degenerates, reflecting the large errors in the upper duct liner, especially for the S_8 calculations.

Figures 5 and 6 show the MCNP and SMHM flux comparisons for the inner and outer liners; the SMHM underpredicts the total fluxes and tends to overpredict the source energy fluxes. At the end of the duct the SMHM underpredicts the flux relative to MCNP; the source energy to total flux ratios are 0.55 and 0.65 for the SMHM and Monte Carlo methods, respectively.

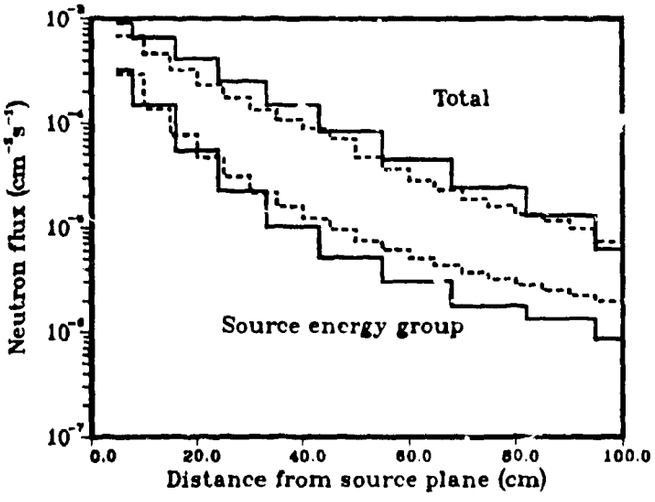

Fig. 6. Flux comparisons in the annular duct inner steel liner as a function of distance from the source plane. (Solid line = MCNP, Dash line = SMHM.)

Summary

Both the cylindrical and annular duct SMHM calculations yield results that are consistent with respect to the MCNP results. In particular, SMHM calculations show a progressive overestimation of the fluxes in the duct steel liner and an underestimation of the flux exiting the duct. Previous studies[2] have indicated that the SMHM approaches from above the analytic uncollided flux in a cylindrical duct, which is opposite to what is observed in this analysis. However, in the previous work scattering was not present.

CONCLUSIONS

The recently developed SMHM method has had an initial testing in two duct streaming problems prototypic of fission and fusion reactor penetrations. Numerical results, when compared to Monte Carlo results, show reasonable agreement in both duct exit and duct wall fluxes. Furthermore, the SMHM provides realistic duct exit fluxes whereas standard discrete-ordinates methods do not. Sources of the observed variation relative to Monte Carlo calculations are proposed, but a clear identification of the contributing factors remains to be made. However, the SMHM appears promising enough, relative to other deterministic methods, that it is being further generalized and tested in TRIDENT-CTR. Specifically, we intend to investigate the effects of cross-section scattering approximations in the duct liners.

REFERENCES

1. Bradley A. Clark, "The Development and Application of the Discrete Ordinates-Transfer Matrix Hybrid Method for Deterministic Streaming Calculations," University of Arizona, Department of Nuclear Engineering, Ph.D. Thesis (1981).

2. Bradley A. Clark, "The Streaming Matrix Hybrid Method for Discrete-Ordinates Calculations," Advances in Reactor Computations, Proc. of an ANS Topical Meeting, Salt Lake City, 28-31 March 1983, p. 135.

3. T. J. Seed, "TRIDENT-CTR User's Manual," Los Alamos Scientific Laboratory report LA-7835-M (May 1979).

4. LASL Group X-6, "MCNP - A General Monte Carlo Code for Neutron and Photon Transport," Los Alamos Scientific Laboratory report LA-7396-M, Rev. (November 1979).

5. R. J. Barrett and R. E. MacFarlane, "The MATXS-TRANSX System and the CLAW-IV Nuclear Data Library," Proc. Int. Conf. on Nuclear Cross Sections for Technology, Knoxville, TN, 22-26 October 1979, National Bureau of Standards Spec. Pub. 594, p. 213.

6. B. G. Carlson, "Tables of Symmetric Equal Weight Quadrature EQ_N Over the Unit Sphere," Los Alamos Scientific Laboratory report LA-4734 (July 1971).

7. G. I. Bell, G. E. Hansen, and H. A. Sandmeier, "Multitable Tretments of Anisotropic Scattering in S_N Multigroup Transport Calculations," Nucl. Sci. Eng. 28, 376 (1967).

8. S. Pelloni, J. Stepanek, and D. J. Dudziak, "Intercomparison of Nuclear Data Library Sources, Group Structures and Collapsing Spectra for INTOR-EC," Proc. Fifth ANS Top. Meeting on Techn. of Fusion Energy, Knoxville, TN, 26-28 April 1983.